Cyanine Polyene Reactivity: Scope and Biomedical Applications

Alexander P. Gorka[1], **Roger R. Nani**[1], **Martin J. Schnermann**[1]

[1]Chemical Biology Laboratory, Center for Cancer Research, National Cancer Institute, Frederick, MD 21702, USA.

Abstract

Cyanines are indispensable fluorophores that form the chemical basis of many fluorescence-based applications. A feature that distinguishes cyanines from other common fluorophores is an exposed polyene linker that is both crucial to absorption and emission and subject to covalent reactions that dramatically alter these optical properties. Over the past decade, reactions involving the cyanine polyene have been used as foundational elements for a range of biomedical techniques. These include the optical sensing of biological analytes, super-resolution imaging, and near-IR light-initiated uncaging. This review surveys the chemical reactivity of the cyanine polyene and the biomedical methods enabled by these reactions. The overarching goal is to highlight the multifaceted nature of cyanine chemistry and biology, as well as to point out the key role of reactivity-based insights in this promising area.

Brief Description

Reactions involving the covalent modification of the cyanine polyene are enabling emerging approaches in optical sensing, super-resolution imaging, and near-IR uncaging.

Graphical Abstract
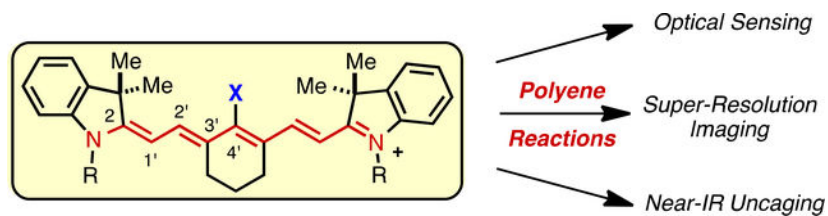
1. Introduction

The rich history of the cyanine class of fluorophores originates with the synthesis of **1** (Fig. 1A) in 1856.[1] Over the intervening years new variants have been developed for use as photographic sensitizers,[2] rewritable DVD response elements,[3] laser dyes,[4] analyte-responsive sensors,[5] and for biomedical fluorescence techniques.[6,7] The indocyanines, which contain a polyene linker connecting 3,3-dialkyl-indolenine heterocycles are generally preferred for biomedical applications. Within this group, the heptamethine cyanines, which contain 7 carbon atoms linking the indolenine heterocycles, are notable because their ~800

martin.schnermann@nih.gov.

nm emission maxima falls in the center of the so-called "near-IR window". Such wavelengths are advantageous for *in vivo* applications as autofluorescence is minimized and light penetration through tissue is maximized. The most medically significant of these is indocyanine green (ICG, **2**), which was first studied over 50 years ago and is an FDA-approved clinical agent initially developed as a blood-pooling agent.[8,9,10] Highlighting the expanding role of near-IR fluorescence in modern diagnostic medicine, new uses for ICG are being examined in over 50 active clinical trials, with especially promising progress achieved in diagnosing lymphoid disorders.[11,12] A variety of indocyanines that lack polyene substitution, including Cy3 (**4**), Cy5 (**5**), Cy7 (**6**), and Alexa 647 (**7**) (Fig. 1B), are commercial products that serve as common biological labels in a range of fluorescence-based experiments.[13,14,15,16] In 1992, a new structural class of heptamethine indocyanines of the general structure **3** (Fig. 1A) was introduced where the polyene region is modified with a heteroatom at C42 and a carbocyclic ring linking C32 and C52.[17] These compounds exhibit generally improved physical properties, greater stability, and higher fluorescence quantum yields compared to ICG.[18,19,20] One commercial derivative, IR800-CW (**8**, Fig. 1B), is being studied extensively for translation as an imaging agent in clinical settings.[21]

The defining chemical feature, and the key chromophore, of the cyanines is the polyene linker. It is perhaps not surprising that this cationic, sterically accessible olefinic functionality is subject to a range of chemical reactions. Maybe more surprising is the extent to which these reactions have be harnessed for productive use. Cyanine polyene reactions have been applied as central components of biomedical techniques in the fields of optical sensing, super-resolution microscopy, and, most recently, near-IR light-mediated uncaging. Here we survey reactions involving the covalent modification of the indocyanine polyene and the resulting applications. We provide a reactivity-driven perspective focused on mechanistic organic chemistry considerations. We anticipate this approach will facilitate the rational design of future applications. Moreover, organizing cyanine polyene reactivity in this fashion may help identify potentially undesirable cross-reactivity at the design stage. To provide the reader with an initial sense for the scope of cyanine polyene reactivity, Figure 1C includes many of the accessible reaction pathways available from the key heptamethine cyanine scaffold.

This review is organized into three sections: (1) reactions associated with chemical sensing and imaging methods, (2) chemical reactivity involved in photoswitching-dependent super resolution microscopy, and (3) photochemical reactions of cyanines and resulting applications. The scope of this review is limited to reactions that covalently modify the polyene linker region or directly attached atoms. Thus, we exclude a series of elegant optical sensing methods that use remote ligand exchange reactions to modify emissive properties through photophysical processes such as photoinduced electron transfer (PET).[22,23,24,25] Aspects of cyanine polyene chemistry have been covered previously in surveys that centered on single-molecule fluorescence,[15,26] cyanine synthesis and stability,[27,28,29] and optical sensing.[22,30,31,32,33,34,35,36,37] This review is the first to systematically organize biologically useful indocyanine polyene reactivity. We hope that this approach will clearly delineate the critical role these reactions play across diverse biological fields and assist in developing future applications of these remarkable molecules.

Section 2.   Cyanine Polyene Reactivity for Optical Sensing

2.1   Background

Fluorogenic small molecules that provide a fluorescent signal in response to an enzymatic process or analyte of interest are integral to a variety of laboratory methods.[38] With coumarin, fluorescein, or rhodamine fluorophores, the general paradigm involves the covalent modification of a key heteroatom (phenol or aniline) by some analyte or enzyme-specific functional group. This added chemical functionality eliminates, or at least reduces, the fluorescence signal and its removal, mediated by the analyte of interest, restores the characteristic emission. Extending these approaches into the near-IR range would facilitate monitoring analytes in blood, tissues, and whole organisms. As the most common near-IR fluorophore, heptamethine cyanines are an obvious candidate scaffold for developing such methods. However, the general approach discussed above is not applicable to conventional cyanine fluorophores. For example, heteroatoms on the indolenine heterocycle do not dramatically influence optical properties as the indolenine ring is outside of the key polyene chromophore. Consequently, the methods below, which involve modification to the cyanine polyene, are born from the necessity of finding alternatives. It is important to mention that a variety of highly useful strategies that rely on the disruption of FRET pairs or the use of PET strategies lie beyond the scope of this survey.[22,39]

2.2   ROS Sensing

Altered levels of reactive oxygen species (ROS) are hallmarks of various disease states and inflammatory processes. Consequently the development of fluorogenic strategies that provide real-time readouts of ROS concentrations are of significant interest.[34] One such strategy uses hydrocyanines (**9**), which are easily formed by sodium borohydride reduction of the terminal C2-N bond in the cyanine polyene (Fig. 2A). Oxidation by various cellular ROS restores the fluorescent cyanine, with particularly rapid kinetics in the case of superoxide ($O_2^{\bullet-}$) and hydroxyl radical ($HO^\bullet$).[40] The oxidation reaction likely proceeds via sequential electron transfer through cyanine radical cation intermediates, however this has not been proven experimentally. Elevated ROS upon angiotensin-mediated oxidative stress was detected in cells and tissues, and in a mouse model involving the lipopolysaccharide (LPS) endotoxin-induced inflammatory response. It was subsequently observed that mono-deuterated variants of hydrocyanines, formed by addition of $NaBD_4$ to the cyanine, display altered reactivity, with distinct kinetic isotope effects (KIE) between background oxidation ($k_H/k_D = 3.7–4.7$) and $O_2^{\bullet-}$ oxidation ($k_H/k_D = 2.6–2.8$).[41] This KIE difference is proposed to improve signal-to-noise ratios and, consequently, provide higher sensitivity for ROS imaging. These molecules are finding extensive use for the detection of ROS in a variety of contexts.[42,43,44,45,46,47,48]

Potent oxidants can, under certain circumstances, react with the cyanine polyene and abolish all long wavelength absorption and emission. A creative approach to ROS sensing takes advantage of this otherwise deleterious process (Fig. 2B).[49] Screening a series of commercially available cyanine fluorophores revealed that the ROS-mediated oxidative reactivity is highly variable and correlates strongly with oxidation potential. For example, IR786S, which bears a thioether at C42, had the lowest measured value (0.303 V) and

reacted most readily with a range of ROS, including with $O_2^{\bullet-}$ and even with high concentrations of H_2O_2, the weakest oxidant tested. Conversely, Cy5SO$_3$H with electron-withdrawing sulfonate groups on the indolenine ring system has the highest oxidation potential (0.628 V) and the greatest resistance to ROS reactivity. The covalent linkage of IR786S ($\Phi_F = 0.035$ with $\lambda_{ex} = 771$ nm) and Cy5SO$_3$H ($\Phi_F = 0.171$ at $\lambda_{ex} = 645$ nm) forms **11**, which exhibits dramatically reduced fluorescence ($\Phi_F = 0.009$ at $\lambda_{ex} = 771$ nm and $\Phi_F = 0.014$ at $\lambda_{ex} = 645$ nm) due to self-quenching. Exposure of **11** to the oxidants peroxynitrite (ONOO$^-$), HO$^{\bullet}$, hypochlorite (ClO$^-$), $O_2^{\bullet-}$, and singlet oxygen ($^1O_2$) provided significant fluorescence enhancements at the Cy5 wavelength. The fluorescence increase arises from the selective oxidation of IR786S to restore the emission of the ROS-resistant fluorophore (Cy5SO$_3$H). Among several applications, $O_2^{\bullet-}$ generated by membrane bound NADPH oxidase was detected in HL60 human promyelocytic leukemia cells. ROS production was also imaged in a mouse model of peritonitis. An important concept that emerges from these efforts is the significant variability in ROS-susceptibility between various cyanines. That is, *certain* cyanines can react with *certain* biologically relevant ROS, whereas other cyanines, for example those with electron-withdrawing groups on the indolenine rings, are nearly immune to such reactions. A detailed description of these oxidative processes, and particularly the specific features that control differential reactivity, would be of significant utility.

The concept of using a ROS-reactive/ROS-resistant pair of fluorophores was extended using highly stable fluorescent semiconducting polymer nanoparticles (SPN) as the ROS-resistant component.[50] SPNs are a new class of arene-based mixed polymeric materials, which provide improved stability as compared to conventional fluorophores or quantum dots. The SPN surface was modified with C42-thiol-substituted heptamethine cyanines, thereby quenching a significant fraction of the SPN fluorescence. Selective oxidation of the heptamethine cyanine by ONOO$^-$, HO$^{\bullet}$, and ClO$^-$ restores much of the lost SPN emission at 678 nm. This approach was used to visualize ROS flux in live murine macrophages and in a mouse model of LPS-induced peritonitis. A hepatocyte-targeted version allowed for real-time monitoring of drug-induced oxidative stress in the liver of live mice.[51] A related polymeric system using rhodamine B as the ROS-resistant element has also been reported.[52] In addition, the oxidation of heptamethine cyanines has also been used as a sensor for hypochlorous acid.[53]

In addition to ROS-sensing, the oxidative reactivity of cyanine fluorophores is the basis for an advanced imaging approach developed by GE.[54] This method, termed multiplexed fluorescence microscopy, uses formalin-fixed paraffin-embedded samples, which is a standard protocol for archiving clinical samples. Cy3 and Cy5-labeled antibodies are applied, subjected to fluorescence microscopy, and then the cyanines are oxidatively inactivated using a proprietary alkaline oxidant mixture, with apparently minimal damage to the samples. This process can be repeated using various antibodies, allowing up to 61 proteins to be visualized in a single sample.

While fluorophores containing the standard cyanine polyene are by far the most common, other cyanine variants have also been studied. Shabat and coworkers recently introduced cyanines modified with an aryl ring in the center of the polyene.[55,56] With conventional

heptamethine cyanines, the two alkylated nitrogen atoms linked through a polyene act as a "donor-acceptor" pair, which is the key chromophore that provides the unique optical properties of these molecules. With these aryl ring incorporated variants, protonation or protection of the phenol forms a dicationic polyene, e.g. **13** (an "acceptor/acceptor" pair) with no meaningful red absorption. Unveiling the phenolate form, which adopts a quinone-methide-like tautomer, e.g. **14**, introduces the key "donor/acceptor" arrangement of the nitrogen atoms thereby providing useful red absorption and emission. The pK_a of the unmasked phenol is 4.5, which means these compounds adopt the fluorescent phenolate form under most biologically relevant conditions. Masking the phenol with a cleavable group creates fluorescent turn-on sensors, which is exemplified here by the selective sensing of H_2O_2 using compound **13** (Fig. 2C). Thus, non-fluorescent **13** is converted to a fluorescent form, **14**, upon boronic acid to phenol oxidation and *p*-quinone methide elimination sequence. It is important to note that the fluorescent form exhibits optical properties ($\Phi_F = 0.16$, $\varepsilon = 5.2 \times 10^4\ M^{-1}\ cm^{-1}$ at 570 nm) that are quite different than the conventional heptamethine cyanine scaffold, although the large Stokes shift may be ideal for certain applications. Nevertheless, these molecules are very promising and a variety of additional applications have been reported since the initial disclosure in 2011, including sensing of nitroreductase,[57] β-galactosidase,[58] cathepsin B,[59] and thiols.[60,61]

A conceptually different approach utilizes analyte-specific cleavage of C42-carbamates to provide C42-amino heptamethine cyanines, which are readily distinguishable by virtue of the hyposochromic shift of the amino variants.[62] Aryl boronic acid or aryl azide cyanines of the structure **15** enable H_2O_2 and H_2S sensing, respectively, with these analytes producing phenols or anilines that undergo intramolecular 1,6-elimination and CO_2 extrusion to provide **16** (Fig. 2D). Simultaneous measurement of the relative fluorescence from the initial carbamate and the product amine enables ratiometric readout. Ratiometric measurement can have certain advantages over simpler turn-on approaches, including greater independence from effects of probe concentration and local environment. Hypsochromic shifts in the absorption and emission of **15a** were only observed in the presence of H_2O_2 among various other ROS, with up to a 22-fold increase in the fluorescence emission. Similar results were obtained with the azide variant **15b**, which showed selectivity for H_2S over other ROS and thiols (F_R/F_{NIR} ~18-fold). The boronic acid derivative **15a** was used to detect exogenous H_2O_2 in fibroblastic NIH 3T3 cells. Treatment of the same cell line with zinc(II) chloride, an H_2S scavenger, ablated the intracellular fluorescence signal of azide **15b** at the blue-shifted emission wavelength.

The detection of lipid peroxides is of significant interest due to the formation of these species during oxidative stress and in a variety of disease states.[63] An unusual approach designed to assess lipid peroxide concentrations was reported using cyanine **17** (Fig. 2E). Compound **17** was formed from a C42-chloro derivative by lithiation with Li(0) and addition of PPh_2Cl to form a C42 C-P bond, presumably followed by phosphine lone pair polyene addition.[64] Occurrence of a polyene reaction was clearly defined by loss of the characteristic cyanine absorption, although a detailed structural assignment using NMR or X-ray crystallography for this quite unusual product has not been reported. Oxidation to form the phosphine oxide **18** with methyl linoleate hydroperoxide (MeLOOH) restores the cyanine

λ_{abs} at 747 nm with concurrent increase in emission. The turn-on effect is selective for ROOH over other ROS and metal ions. Exposure to *t*-Bu and cumene hydroperoxides did not lead to a restoration of cyanine absorption and emission, suggesting that **17** may be particularly selective for unhindered organic hydroperoxides. Oxidative stress induced by stimulation of macrophages with a phorbol ester was analyzed using **17**. A related probe involving C42-selenium substitution has also been reported.[65,66]

The potential for environmental alkyl mercury toxins to induce neurotoxicity have created a need for improved sensing methods.[67] One such approach involves a methyl mercury-induced cyclization of the C42 amine, **19**, on a pendant thiourea to form a cyclic guanidine (**20**, Fig. 2F).[68] Related mercury-mediated cyclization reactions have been used elsewhere for sensing-applications.[69] Mercury salts selectively promote this cyclization, with little competing reactivity from cadmium, silver, copper, and lead salts. The reaction converts the blue-shifted amine derivative ($\lambda_{abs} = 670$ nm) to a C42-guanidine derivative ($\lambda_{abs} = 810$ nm), allowing for efficient ratiometric sensing and cellular fluorescence imaging.

2.3 pH Sensing

Many approaches have been explored for the generation of pH-sensitive fluorescent molecules.[70] To extend these techniques into the near-IR range, several have used the protonation of C42-amino heptamethine cyanines. This category includes the use of a C42-*m*-amino-phenol derivative, **21** (Fig. 3A).[71] Compound **21** displays a fairly complex pH profile, likely due to the presence of two titratable protons, with a useful 10-fold increase in fluorescence intensity within a pH range of 4.0–6.5. Another method uses C42 piperidine derivatives, such as **23** (Fig. 3B).[72] Here, the far-red absorption of the unprotonated form is converted to a near-IR absorption upon protonation. The distinct absorption spectra enabled ratiometric sensing, which increased the sensitivity of these measurements. Compounds **21** and **23** both capitalize on altering the capacity of the central C42-amine lone pair to donate electron density into the cyanine polyene. C42-free amines exhibit an atypical cyanine absorption with a significantly hypsochromically-shifted absorption spectra, whereas the protonated forms more closely resemble other C42 derivatives (e.g. *Cl*-, *O*-, *C*-, or *S*-). Another recent elegant approach used heptamethine cyanines substituted at C42 with a pyrazole heterocycle.[73]

The cellular internalization of many tumor-targeting agents is accompanied by significant reduction of the local pH as the targeting agent/receptor complex is trafficked through endosomal compartments to the lysosome. An approach to selectively report on ligand/receptor internalization was recently disclosed by Achilefu and coworkers. These studies employ a heptamethine cyanine labeled the with the $\alpha_v\beta_3$ integrin-avid peptide cRGD, **25**, that undergoes fluorescence enhancement in acidic environments (Fig. 3C).[74] The pH sensitivity of **25** is derived from the norcyanine scaffold, which bears unsubstituted, as opposed to alkylated, indolenine nitrogen atoms. The molecule exhibits a characteristic heptamethine cyanine absorption and emission only upon protonation of the indolenine nitrogen (pK_a ~ 4.7). At neutral pH, the absorption of the uncharged cyanine is dramatically shifted to the visible region ($\lambda_{abs} \approx 520$ nm). The cRGD peptide-$\alpha_v\beta_3$ integrin receptor interaction led to selective trafficking to late endosomal/lysosomal compartments in MDA-

MB-435 and 4T1/*luc* cells *in vitro*. Productive imaging was further demonstrated in a 4T1/*luc* orthotopic tumor model. A related approach has also been investigated using pentamethine cyanines.[75]

2.4 Thiol Sensing

Thiols, particularly cysteine (Cys), homocysteine (Hcy), and glutathione (GSH), play important roles in redox homeostasis, and diminished thiol regulation is implicated in several disorders and disease states.[76] A variety of approaches to thiol sensing have been developed using the unique chemistry of the C42 position of heptamethine cyanines. One such approach for selective sensing of intracellular Cys uses **27**, which is functionalized with an acrylate ester at C42 (Fig. 4A).[77] Cysteine addition forms a Michael-addition adduct that rapidly cyclizes/eliminates to afford the C42-ketone **28**. The absorption spectrum of the product **28** is hypsochromically-shifted relative to **27** and, consequently, can be measured almost independently with the resulting ratio representing reaction progress. The rate of ketone formation with Cys is approximately tenfold greater than that of Hcy, likely owing to increased kinetics for forming the cyclic intermediate (seven-membered ring formation faster than eight). Intracellular Cys levels were examined *in vitro* using MCF-7 cells cultured in standard and glucose-deficient environments, which elevates both GSH and its precursor, Cys, due to oxidative stress. [78] A conceptually related strategy for H_2S sensing using **29** also was recently reported (Fig. 4B).[79] Nucleophilic addition of hydrogen sulfide to the aldehyde triggers a second nucleophilic addition to the ester to provide the corresponding C42-ketone **30**. The probe displays selectivity toward H_2S over other thiol-containing molecules, such as Cys and GSH, and exhibits a linear correlation between fluorescence enhancement at 625 nm and H_2S concentration with a detection limit of 10 nM. Neither of these C42 cyanine esters have been applied in animal models, and it is possible that premature ester-to-ketone conversion, perhaps through hydrolysis or esterase activity, precludes live animal applications. Notably, the pK_a of the ketone product, ~4.5, should be considered when contemplating the reactivity of these compounds.[80] Along these lines, a simple C42-acetylated derivative was used as an esterase-activated probe.[81] A nearly identical molecule has also been reported to be a hydrazine sensor.[82]

Another approach to thiol sensing sought to address the key role of mitochondrial thiol regulation, an important area given the central role of mitochondria in ROS generation and cellular redox signaling.[83] In particular, the mitochondrial glutathione (mGSH) pool is a critical antioxidant reservoir that protects mitochondrial proteins from oxidative stress generated during normal aerobic metabolism.[84] Therefore, a near-IR fluorescent probe capable of localizing to mitochondria and distinguishing mGSH from other thiols (e.g. Cys and Hcy) would be of significant utility. A heptamethine cyanine, **31**, was recently reported as a probe for selective sensing of mGSH (Fig. 4C).[85] In this design, the cationic heptamethine system of **31** in concert with the relatively hydrophobic *n*Bu esters leads to selective mitochondrial targeting. Meanwhile, the C42-diaryldiazoether serves as a fluorescence quencher via PET that is interrupted by GSH-selective reactivity to form the GSH-incorporated product **32**. A measureable "turn-on" effect was observed upon exposure to GSH at concentrations as low as 26 nM. NMR analysis using β-mercaptoethanol support a mechanism in which C42-thiolate nucleophilic substitution leads to loss of the

diaryldiazoether functionality, thereby interrupting PET quenching. Evidence is provided that, unlike thiol addition in organic solvents (which proceeds through a $S_{RN}1$ mechanism), [17] the thiolate nucleophilic substitution reaction in protic conditions proceeds through an ionic reaction pathway. Specifically, a 10-fold rate enhancement was observed in protic solvent (methanol) over aprotic solvent (DMSO), while addition of a radical scavenger (O_2) and an electron scavenger (nitrobenzene) had no effect. The fluorescence signal from **31** at 810 nm increased approximately 450-fold in the presence of GSH, while exposure to two other biologically relevant thiols, Cys and Hcy, shifted the emission maximum to 747 nm and only resulted in a 10- and 15-fold fluorescence enhancement, respectively. This dramatic selectivity results from the C42-substitution adducts formed from Cys and Hcy undergoing subsequent intramolecular cyclization to provide a C42-*N*-linked product, **33** (Fig. 4C). A recent synthesis-oriented study observed a similar intramolecular cyclization.[86] Notably, mitochondrial localization was derived specifically from the *n*-Bu ester functional group, as the corresponding carboxylic acids and *N*-(2-morpholinoethyl)amides induced cytosolic and lysosomal accumulation, respectively. The sensing reaction was shown to be dependent on mGSH levels, as "turn-on" fluorescence intensity decreased in the presence of GSH scavengers and increased in the presence of GSH enhancers. A related approach has been reported for hydrogen sulfide sensing using the conversion of a C42-chloro cyanine, which displays significant fluorescence, to the nonfluorescent C42-free thiol form.[87]

A fundamental understanding regarding the timing of cellular internalization and drug release could provide key insights useful for drug development. A fluorogenic strategy using **34** provided a fluorescent readout for intracellular accumulation and drug release (Fig. 4D) through a method based on the elevated cellular thiol concentrations.[88] The design of this approach relies on another instance of distinguishing a C42-amino fluorophore from one with a less π-donating C42 substituent. In this case, the amine exhibits a significant detectable emission when excited at 615 nm, whereas the carbamate variant has only modest emission when excited at the same wavelength. Compound **34** contains a C42-carbamate linked through a disulfide to a carbamate modified version of gemcitabine, a nucleoside analogue currently used as a broad spectrum chemotherapeutic.[89] The cyanine scaffold was also appended with a folate-targeting ligand to enable selective uptake in cells over-expressing the folate receptor. Intracellular disulfide cleavage and intramolecular cyclization cleaves the C42-carbamate to provide the C42-amine, **36**, creating the fluorescence "turn-on" effect (Fig. 4D). Concurrently, a similar process unmasks the 52-hydroxyl of gemcitabine, **35**, affording the active drug molecule. The disulfide linkage is cleaved by thiols, with an approximately 40-fold fluorescence enhancement observed for **34** in the presence of GSH and negligible increase in the presence of nonthiol-containing amino acids and metal ions. Reduction of intracellular thiols using *N*-ethylmaleimide, a thiol-reactive electrophile, attenuates the turn-on effect. This approach was used to evaluate the receptor-mediated cellular internalization of **34** in folate receptor (FR)-positive KB cells and not FR-negative cells in both *in vitro* and *in vivo* experiments.

2.5   Other Methods

While the majority of cyanine polyene chemistry useful for sensing applications involves heptamethine cyanines, there are isolated examples of reactions in other systems. In

particular, it has been observed that hybrid indocyanine/coumarin dyes react with biologically relevant nucleophiles at the electrophilic indolenine position. One such approach involves compound **37**, which was applied towards the detection of mitochondrial H_2S (Fig. 5A).[90] Nucleophilic addition of HS^- at the C2-indolenine carbon to form **38**, which was confirmed by NMR, abolishes merocyanine emission while leaving the coumarin emission unaffected. The resulting ratiometric measurement was quite selective for H_2S (pK_a ~7) over Cys, GSH, Hcy, and bovine serum albumin (pK_as 8.5). **37** preferentially localizes to the mitochondria in MCF-7 cells and was used for the ratiometric visualization of exogenous H_2S. A closely related strategy has been explored for cyanide sensing.[91,92]

Fluorescent complexes formed from the combination of encoded proteins and exogenously supplied small molecules can provide unique optical properties and a level of temporal and spatial control not possible with conventional fluorescent proteins alone.[93] For example, SNAP- or Halo-tag approaches allow suitably modified fluorophores to be affixed to nearly any protein through the genetic incorporation of the tagging complex.[94] An exciting contribution to this rapidly expanding field involves the nucleophilic addition of a lysine residue on an engineered protein to a non-fluorescent cyanine precursor, **39**, to form a fluorescent cyanine/protein complex *in situ* (Fig. 5B). [95] As one might expect, fluorescence requires the protonated form of the Schiff base, which predominates under most biologically relevant conditions due to its pK_a of 9.6. The protein reengineering process used cellular retinoic acid binding protein II (CRABPII), a retinoic acid carrier protein, as the starting point. The design of this approach was stimulated by the structural homology between the cyanines and the retinoids, and capitalized on recent studies from the same group dealing with rational modification of CRABPII/retinal complexes.[96,97]

Section 3. Cyanine Polyene-Based Switching for Super Resolution Microscopy

Super resolution methods that exceed the diffraction limit are revolutionizing fluorescence microscopy.[98,99,100,101] Among several general approaches, one set of methods relies on imaging single molecules undergoing controlled switching between dark and emissive states. By collecting photons from a few single-molecule emitters, which represent only a fraction of all the labels in the sample, sub-diffraction limit resolution can be achieved by calculating the center of the single-molecule emission pattern (generally assumed to be a simple Gaussian distribution) prior to its return to a dark state. Repeated activation, localization, and deactivation forms a high-resolution pattern (Fig. 6A). The two most common methods of this type are referred to as photoactivated localization microscopy (PALM), which generally involves photoactivateable fluorescent proteins, and stochastic optical reconstruction microscopy (STORM), which usually employs cyanine fluorophores (particularly Alexa 647). While key aspects of these methods span numerous scientific disciplines, with many details residing beyond the scope of this review, a critical component is the chemistry controlling the pivotal on/off events.[102,103] The chemistry of cyanine photoswitching, which featured prominently in the early methodological developments and is still a pillar of these approaches, has been elucidated to a detailed molecular level and is reviewed below.

The propensity of cyanines, particularly pentamethine variants, to reversibly enter relatively long-lived dark states at the single molecule level was observed in early single molecule spectroscopy studies.[104,105] These blinking events can be controlled by altering between 488 nm (on) and 633 nm (off) light, and require efficient oxygen removal and high concentrations (mM) of a primary thiol. The utility of this observation for super resolution imaging (as STORM) was subsequently developed by Zhuang and coworkers.[106,107] Subsequently, the blinking phenomenon was shown to involve light-mediated primary thiolate addition to C22 of the pentamethine cyanine polyene (Fig. 6Ba).[108] Thus, illumination of a pentamethine cyanine derivative (**41**) at 633 nm in the presence of β-mercaptoethanol (βME) decreased the near-IR absorption at 650 nm due to the formation of a thiol-cyanine adduct (**42**). UV irradiation restores the intact cyanine and its 650 nm absorption. Preferential thiol addition to C22 on a model pentamethine cyanine was demonstrated by MS/MS analysis. Mechanistically, the reaction is proposed to involve initial formation of a cyanine-thiolate encounter complex, excitation, and final thiolate addition, with the key thiolate addition step likely involving an initial electron transfer followed by thiyl radical addition. The rate of switching to the dark state initially increases linearly (first-order kinetics) and saturates above 1 M βME concentration (zero-order kinetics), and the reaction rate is reduced in the presence of a radical quencher (isoascorbate). Consistent with the overall reaction model, blinking is also effective using other primary thiols (β-mercaptoethylamine and Cys derivatives), and, in recent work, the high intracellular GSH concentration has enabled live-cell imaging without the addition of thiol-containing buffers. [109] This process is compatible with pentamethine cyanines and heptamethine cyanines, but not trimethine cyanines. A recent detailed analysis provided a comprehensive examination of the applicability of various commercial fluorophores to this method.[110] Of note, while thiol adducts of heptamethine cyanines have been observed using mass spectral analysis,[108] the site of reactivity (i.e. which carbon is modified in the polyene chain) has not been determined. Critically, with other classes of fluorophores, and possibly with certain cyanines, dark states arise through redox events to form non-fluorescent radical intermediates.

It has also been demonstrated that relatively stable dark states can be generated through phosphine addition to the cyanine polyene (Fig. 6Bb).[111] Exposure of Cy5 to millimolar concentrations of tris(2-carboxyethyl)phosphine (TCEP), a widely used reducing agent, leads to rapid formation of a phosphine adduct, **43**. In contrast to the thiol addition discussed above, this reaction occurs spontaneously in the absence of light, with UV irradiation in this case restoring the intact cyanine polyene. Kinetic analysis supports a reversible bimolecular reaction model, with $K_{eq} = 0.91$ mM^{-1}. Convincing mass spectral and ^{1}H NMR evidence for TCEP addition to C22 of the pentamethine polyene has been obtained. As above, other pentamethine and heptamethine variants were also reversibly quenched by TCEP, however trimethine cyanines were again unaffected. This approach enabled two-color STORM imaging using a combination of Alexa 647 and Alexa 750.

Another method to generate stable dark states for super resolution imaging uses the reduced form of cyanines, the hydrocyanines, which were discussed in Section 2.2 for ROS sensing. [112] Treatment of a variety of cyanine dyes with sodium borohydride results in hydride

addition to the indolenine carbon, causing a large blue shift that leaves the resulting hydrocyanine (**44**) in an effective "dark" state (Fig. 6Bc). Subsequent illumination with UV or violet light recovers a variable percentage of the reduced dye molecules to the fluorescent state, enabling STORM imaging. The rate of the oxidation process can be enhanced through the use of riboflavin, which acts as a photosensitizer in the presence of UV light to generate cyanine-activating ROS. Low recovery yields represent a limitation of this approach, but this can be somewhat compensated for by increasing the degree of labeling. The biologically compatible oxidation of hydrocyanines to cyanines illustrates how useful reaction-based insights can be. These two different applications, ROS-sensing (discussed in Section 2.2) and STORM activation, are totally distinct at a cursory glance but, nevertheless, involve the same enabling chemical transformation.

An active area of research is the development of small molecules designed to photoswitch spontaneously. One chemical approach towards this goal is based on hybrid coumarin/cyanines such as **45** (Fig 6Bd).[113] The pendant phenol, which preferentially forms the ring-closed oxazine form **46**, opens (on-state, **45**) upon UV illumination on a subnanosecond timescale and spontaneously reverts to the ring-closed isomer (off-state) on a submicrosecond timescale. The ring-open state can be trapped by protonation of the resulting phenolate. The concept of using a pendant nucleophile for photoswitching was also recently reported on the rhodamine scaffold.[114]

4. Photochemistry of the Cyanine Polyene and Resulting Applications

4.1 Cyanine Photooxidation - Background

As with most fluorophores, cyanines are susceptible to light-dependent decomposition or photobleaching, which can be deleterious for a variety of fluorescence experiments. Starting with a seminal study by Byers at the Kodak laboratories in 1976, a several studies examined the chemical basis of this photodegradation process.[115] As observed across several structurally desperate cyanine scaffolds, photolysis results in oxidative C-C cleavage occurring at certain positions along the polyene chain.[116,117,118,119,120,121,122,123] Representative of this cleavage reaction is the conversion of ICG to products **47** to **50** (Fig. 7A). The most common mechanism to describe this process involves photosensitization to form $^1O_2$, dioxetane formation, and final dioxetane cleavage to form carbonyl products (Fig. 7B). Key pieces of evidence to support this pathway include: (1) a dependence on oxygen concentration,[117] (2) decreased, though not completely ablated, kinetics in the presence of $^1O_2$ quenchers (e.g. NaN_3),[120] (3) accelerated kinetics in deuterated solvents which extend the lifetime of singlet oxygen,[124] (4) the use of singlet oxygen trapping agents,[118,124] and (5) the direct observation of dioxetane intermediates by mass spectrometry (+32 mass units).[120,123] It is important to note that cyanine photobleaching may involve alternative pathways to that presented in Figure 7.[118,122,125] The most likely alternative mechanism involves electron transfer, rather than energy transfer, from the triplet state. Electron transfer with oxygen would produce both $O_2^{\bullet-}$, which may ultimately generate $HO^{\bullet}$ or other ROS, and the potentially reactive cyanine-radical cation. Critically, the products resulting from this alternative pathway, and the substrates or circumstances that favor it, remain to be defined. A

detailed understanding of the interplay between these two possible mechanisms, as well as a quantitative accounting of the products formed through photolysis, is still required.

4.2 Approaches to Circumvent Cyanine Photooxidation

Several strategies have been developed to reduce the photobleaching rate of cyanines.[126] One general approach is to introduce electron-withdrawing groups that remove electron density from the polyene, presumably to reduce the kinetics of $^1O_2$ reactions. Perfluorination of the aromatic rings of thiadicarbocyanine **51** to provide **52** appreciably reduced aggregation and photobleaching (by ~3.5-fold) compared to the all protio counterpoint, although with somewhat reduced molar absorptivity (Fig. 8A).[121] Alternatively, the cyano-substituted merocyanine **54** displayed a reduced rate (~39-fold) of photobleaching versus the analogue, **53**, that lacks the electron-withdrawing functionality (Fig. 8B).[122] Exogenously generated $^1O_2$ (formed by methylene blue photosensitization) reacted with the original merocyanine **53**, but not with **54**. The fact that **54** photobleaches at all, despite being apparently immune to exogenously-generated $^1O_2$, is evidence for $^1O_2$ independent pathways in the photobleaching of, at least some, cyanines.

Stable emission profiles are particularly critical for single molecule fluorescence experiments and a variety of efforts have addressed cyanine photobleaching in this context. Oxygen removal, through enzymatic methods, reduces the rate of irreversible bleaching but leads to rapid (ms) intensity fluctuations (blinking) due to long-lived triplet states.[26] Triplet quenchers (such the hydroquinone, Trolox, and cyclooctatetraene) have been added to mounting media to mitigate blinking. These triplet quenchers both reduce dark states and decrease the rate of photobleaching.[127] Building on the use of these molecules as antifade additives, Blanchard and coworkers recently introduced the concept of "self-healing" cyanines, which involves the covalent linkage of a triplet state-quenching group (TSQ) tethered to a pentamethine cyanine (**56**, Fig. 8C).[125,128,129] It was demonstrated, in both bulk and single molecule fluorescence experiments, that the appended TSQ (nitrobenzyl, cyclooctatetraene, or Trolox) improves photostability. In the absence of oxygen removal in bulk solution there was approximately a 7-fold improvement with nitrobenzyl and cyclooctatetraene modification and approximately a 2-fold improvement with Trolox modification, with greater stability improvements observed with enzymatic oxygen depletion. The ability of proximate triplet quenchers to improve cyanine photostability has also been investigated using DNA templating.[130,131]

4.3 Cyanine Photooxidation for Near-IR Uncaging

Much as near-IR fluorescence is required for many live-animal imaging applications, near-IR photocaging methods are required to advance the photocaged/uncaged logic into organismal contexts. There has been significant progress using two-photon approaches, which are ideally suited for rapid uncaging in the small focal volumes achieved with pulsed femtosecond laser sources, and in thermal-release methods usually involving metallic nanoparticles. [132,133,134,135] Existing single-photon photochemistry initiated by light of longer wavelengths is quite sparse, especially when compared to the variety of available lower wavelength approaches, with only a handful of reports just appearing in recent years. [136,137,138,139,140,141]

The photochemical reactivity of heptamethine cyanines discussed above, coupled with their well-established biocompatibility, suggested to us that these fluorophores might have a second use as a platform for near-IR uncaging. A first foray into this area led to an approach using C42-amine-linked heptamethine cyanines of the general type **57** (Fig. 9).[123] We projected that the key bond breaking event would occur through the selective hydrolysis of the C42-*N* bond in photooxidation products **58** and **59** but not in the starting compound **57**. The motivating notion was that altered π-conjugation would increase the electrophilic reactivity of the key C42-*N* bond (i.e. through the increased iminium character). As shown in Figure 9A, the overall reaction sequence comprises photosensitization to form $^1O_2$, formation of dioxetanes, dioxetane cleavage to from the hydrolytically labile intermediates **58** and **59**, and final hydrolysis/cyclization to provide the uncaged phenol. The release reaction was characterized by NMR, absorption, fluorescence, and mass spectrometry methods. Remarkably, each of the key intermediates are observable by mass spectral analysis, and time-course studies validated the general mechanistic model. These compounds display excellent dark stability, the photochemical reactions can be initiated by a convenient, low-energy 690 nm LED light source, and the chemistry proceeds readily under a variety of conditions. In proof-of-concept applications, this method was used to inhibit cell viability through the light-dependent release of the estrogen receptor antagonist, 4-hydroxycyclofen, using cyanine **57C** (Fig. 9B,C). We also demonstrated, through uncaging of the same compound, near-IR light mediated control of gene expression in a ligand-dependent CreER^T/LoxP-reporter cell line.[142] One advantageous component of this method is that the fluorescence of these compounds can be used to evaluate pre-uncaging localization with low light fluence, prior to applying high fluence for small molecule delivery. Thus, this photooxidation of heptamethine cyanines, originally associated only with fluorophore degradation, has a promising second career as the centerpiece of a new approach for near-IR uncaging.

Conclusion

Molecules containing the cyanine scaffold are fundamental components of many experimental biological procedures and clinical diagnostic protocols. As detailed above, reactions involving the exposed cyanine polyene play pivotal roles in a number of emerging biomedical methods. While cyanines themselves are not new, reactions of the cyanine polyene are almost all quite recent. A promising component of many of these emerging techniques is the use of heptamethine cyanines. The near-IR optical properties of these molecules render these approaches excellent candidates for translation into complex animal and, ultimately, clinical settings. The recent clinical success of fluorescence-guided surgery clearly underscores the potential of near-IR optical methods.[143]

The biological utility of these molecules rests, by necessity, on a chemical foundation. Quite notably, several of the methods discussed above were discovered by identifying a productive use for molecular events that could have easily been seen as only detrimental to standard imaging applications (e.g. oxidative polyene cleavage for ROS sensing, single molecule blinking for super resolution microscopy, and photooxidation for near-IR uncaging). The conversion of these undesirable, typically loss of signal events, into useful procedures was facilitated by a mechanistic understanding of the underlying chemistry. Future efforts will

need to define approaches that modulate and distinguish between the various, likely sometimes competing, reaction pathways. Consequently, interdisciplinary efforts that blend physical organic chemistry, complex molecule synthesis, and advanced chemical biology and biomedical techniques are essential.

Acknowledgments

Biographies

Alexander Gorka earned his B.S. in Chemistry in 2008 from Monmouth University, NJ. He went on to obtain a Ph.D. in Chemistry under Prof. Paul Roepe at Georgetown University, where he studied drug pharmacology and resistance in *Plasmodium falciparum* malaria. He is currently a postdoctoral fellow with Dr. Martin Schnermann in the Chemical Biology Laboratory at the National Cancer Institute, working on developing and applying near-IR light-based uncaging strategies for drug delivery and control of gene expression.

Roger Nani graduated from Boston College in 2006 with a B.S. degree in Biochemistry. After working at Amgen in Cambridge, MA he joined Professor Sarah E. Reisman's group at the California Institute of Technology, earning a Ph.D. in Organic Chemistry in 2013. He is currently engaged in postdoctoral research with Dr. Martin J. Schnermann in the Chemical Biology Laboratory at the National Cancer Institute, working on the discovery of near-IR light uncaging methods using heptamethine cyanine photochemistry.

Martin Schnermann is an investigator in the Chemical Biology Laboratory in the intramural program of the National Cancer Institute (NCI). He attended Colby College and graduated in 2002 with degrees in Chemistry (research with Prof. Dasan Thamattoor) and Physics. After a year at Pfizer, he was a graduate student Prof. Dale Boger at the Scripps Research Institute and obtained his Ph.D. in 2008. He then completed an NIH-postdoctoral fellowship with Prof. Larry Overman at the University of California, Irvine. In 2012, Dr. Schnermann joined the NCI where his research focuses on the development of new chemical approaches for drug delivery and imaging, as well as the synthesis of natural products of relevance to cancer imaging and therapy.

Picture

Roger Nani (Right), Alex Gorka (Center), Martin Schnermann (Left)

References

1. Williams CHG, Trans. Roy. Soc. Edinburgh 1856, 21, 377.

2. Lenhard JR, Hein BR and Muenter AA, J. Phys. Chem, 1993, 97, 8269.

3. Mustroph H, Stollenwerk M and Bressau V, Angew. Chem. Int. Ed, 2006, 45, 2016.

4. Fabian J, Nakazumi H and Matsuoka M, Chem. Rev, 1992, 92, 1197.

5. Yuan L, Lin WY, Zheng KB, He LW and Huang WM, Chem. Soc. Rev, 2013, 42, 622. [PubMed: 23093107]

6. Luo SL, Zhang EL, Su YP, Cheng TM and Shi CM, Biomaterials, 2011, 32, 7127. [PubMed: 21724249]

7. Pansare VJ, Hejazi S, Faenza WJ and Prud'homme RK, Chem. Mater, 2012, 24, 812. [PubMed: 22919122]

8. Busch DR and Chance B, Diffuse Optical Tomography and Spectroscopy in Molecular Imaging Principles and Practice, Weissleder R, Ross BD, Rehemtulla A and Gambhir SS, Eds.; Peoples: Connecticut, 2010; p. 214–215.

9. Frangioni JV, Curr. Opin. Chem. Biol 2003, 7, 626. [PubMed: 14580568]

10. Alford R, Simpson HM, Duberman J, Hill GC, Ogawa M, Regino C, Kobayashi H and Choyke PL, Mol. Imaging, 2009, 8, 341. [PubMed: 20003892]

11. From https://clinicaltrials.gov, search term ICG.

12. Marshall MV, Rasmussen JC, Tan IC, Aldrich MB, Adams KE, Wang X, Fife CE, Maus EA, Smith LA and Sevick-Muraca EM, Open. Surg. Oncol. J, 2010, 2, 12. [PubMed: 22924087]

13. Ernst LA, Gupta RK, Mujumdar RB and Waggoner AS, Cytometry, 1989, 10, 3. [PubMed: 2917472]

14. Mujumdar RB, Ernst LA, Mujumdar SR, Lewis CJ and Waggoner AS, Bioconjug. Chem, 1993, 4, 105. [PubMed: 7873641]

15. Stennett EMS, Ciuba MA and Levitus M, Chem. Soc. Rev, 2014, 43, 1057. [PubMed: 24141280]

16. Ye Y, Li WP, Anderson CJ, Kao J, Nikiforovich GV and Achilefu S, J. Am. Chem. Soc, 2003, 125, 7766. [PubMed: 12822971]

17. Strekowski L, Lipowska M and Patonay G, J. Org. Chem, 1992, 57, 4578.

18. Patonay G, Kim JS, Kodagahally R and Strekowski L, Appl. Spectrosc, 2005, 59, 682. [PubMed: 15969815]

19. Strekowski L, Lipowska M, Gorecki T, Mason JC and Patonay G, J. Heterocyclic. Chem, 1996, 33, 1685.

20. Tarazi L, George A, Patonay G and Strekowski L, Talanta, 1998, 46, 1413. [PubMed: 18967271]

21. Marshall MV, Draney D, Sevick-Muraca EM and Olive DM, Mol. Imaging Biol, 2010, 12, 583. [PubMed: 20376568]

22. Yuan L, Lin WY, Zheng KB, He LW and Huang WM, Chem. Soc. Rev, 2013, 42, 622. [PubMed: 23093107]

23. Que EL, Domaille DW and Chang CJ, Chem. Rev, 2008, 108, 1517. [PubMed: 18426241]

24. Sasaki E, Kojima H, Nishimatsu H, Urano Y, Kikuchi K, Hirata Y and Nagano T, J. Am. Chem. Soc, 2005, 127, 3684. [PubMed: 15771488]

25. Li Y, Sun Y, Li J, Su Q, Yuan W, Dai Y, Han C, Wang Q, Feng W and Li F, J. Am. Chem. Soc, 2015, DOI: 10.1021/jacs.5b04097.

26. Levitus M and Ranjit S, Q. Rev. Biophys, 2011, 44, 123. [PubMed: 21108866]

27. Henary M and Mojzych M, Stability and Reactivity of Polymethine Dyes in Heterocyclic Polymethine Dyes: Synthesis, Properties and Applications; Strekowski L Ed.; Topics in Heterocyclic Chemistry 14; Springer-Verlag: Berlin; 2008, pp. 221.

28. Panigrahi M, Dash S, Patel S and Mishra BK, Tetrahedron, 2012, 68, 781.

29. Mishra A, Behera RK, Behera PK, Mishra BK and Behera GB, Chem. Rev, 2000, 100, 1973. [PubMed: 11749281]

30. Yin J, Hu Y and Yoon J, Chem. Soc. Rev, 2015, DOI 10.1039/C4CS00275J.

31. Guo ZQ, Park S, Yoon J and Shin I, Chem. Soc. Rev, 2014, 43, 16. [PubMed: 24052190]

32. You Y and Nam W, Chem. Sci, 2014, 5, 4123.

33. Lippert AR, J. Inorg. Biochem, 2014, 133, 136. [PubMed: 24239492]

34. Chen X, Tian X, Shin I and Yoon J, Chem. Soc. Rev, 2011, 40, 4783. [PubMed: 21629957]

35. Lin VS, Chen W, Xian M, Chang CJ, Chem. Soc. Rev, 2015, DOI 10.1039/C4CS00298A.

36. Singha S, Kim D, Seo H, Cho SW and Ahn KH, Chem. Soc. Rev, 2015, DOI: 10.1039/C4CS00328D

37. Singha S, Kim D, Moon H, Wang T, Kim KH, Shin YH, Jung J, Seo E, Lee S-J and Ahn KH, Anal. Chem, 2015, 87, 1188. [PubMed: 25495776]

38. Grimm JB, Heckman LM and Lavis LD, Prog. Mol. Biol. Transl. Sci, 2013, 113, 1. [PubMed: 23244787]

39. Fan J, Hu M, Zhan P and Peng X, Chem. Soc. Rev, 2013, 42, 29. [PubMed: 23059554]

40. Kundu K, Knight SF, Willett N, Lee S, Taylor WR and Murthy N, Angew. Chem. Int. Ed, 2009, 48, 299.

41. Kundu K, Knight SF, Lee S, Taylor WR and Murthy N, Angew. Chem. Int. Ed, 2010, 49, 6134.

42. Kim JY, Choi WI, Kim YH and Tae G, J. Control. Release, 2011, 156, 398. [PubMed: 21787816]

43. Yuan L, Lin W and Song J, Chem. Commun, 2010, 46, 7930.

44. Swanson II PA, Kumar A, Samarin S, Vijay-Lumar M, Kundu K, Murthy N, Hansen J, Nusrat A and Neish AS, Proc. Natl. Acad. Sci. U S A, 2011, 108, 8803. [PubMed: 21555563]

45. Selvam S, Kundu K, Templeman KL, Murthy N and J Garcia A, Biomaterials, 2011, 32, 7785. [PubMed: 21813173]

46. Magalotti S, Gustafson TP, Cao Q, Abendschein DR, Pierce RA, Berezin MY and Akers WJ, Mol. Imaging. Biol, 2013, 15, 423. [PubMed: 23378226]

47. Goodson P, Kumar A, Jain L, Kundu K, Murthy N, Koval M and Helms MN, Am. J. Physiol. Lung Cell. Mol. Physiol, 2012, 302, L410. [PubMed: 22160304]

48. Suri S, Lehman SM, Selvam S, Reddie K, Maity S, Murthy N and Garcia AJ, J. Biomed. Mater. Res. A, 2015, 103A, 76.

49. Oushiki D, Kojima H, Terai T, Arita M, Hanaoka K, Urano Y and Nagano T, J. Am. Chem. Soc, 2010, 132, 2795. [PubMed: 20136129]

50. Pu K, Shuhendler AJ and Rao J, Angew. Chem. Int. Ed, 2013, 52, 10325.

51. Shuhendler AJ, Pu K, Cui L, Uetrecht JP and Rao J, Nat. Biotechnol, 2014, 32, 373. [PubMed: 24658645]

52. Chen G, Song F, Wang J, Yang Z, Sun S, Fan J, Qiang X, Wang X, Dou B and Peng X, Chem. Commun, 2012, 48, 2949.

53. Lou Z, Li P, Song P and Han K, Analyst, 2013, 138, 6291. [PubMed: 23986031]

54. Gerdes MJ, et al., Proc. Natl. Acad. Sci. U S A, 2013, 110, 11982. [PubMed: 23818604]

55. Karton-Lifshin N, Segal E, Omer L, Portnoy M, Satchi-Fainaro R and Shabat D, J. Am. Chem. Soc, 2011, 133, 10960. [PubMed: 21631116]

56. Karton-Lifshin N, Albertazzi L, Bendikov M, Baran PS and Shabat D, J. Am. Chem. Soc, 2012, 134, 20412. [PubMed: 23194283]

57. Shi YM, Zhang SC and Zhang XR, Analyst, 2013, 138, 1952. [PubMed: 23420121]

58. Karton-Lifshin N, Vogel U, Sella E, Seeberger PH, Shabat D and Lepenies B, Org. Biomol. Chem, 2013, 11, 2903. [PubMed: 23519143]

59. Kisin-Finfer E, Ferber S, Blau R, Satchi-Fainaro R and Shabat D, Bioorg. Med. Chem. Lett, 2014, 24, 2453. [PubMed: 24767838]

60. Maity D and Govindaraju T, Org. Biomol. Chem, 2013, 11, 2098. [PubMed: 23306953]

61. Redy-Keisar O, Kisin-Finfer E, Ferber S, Satchi-Fainaro R and Shabat D, Nat. Protocol, 2014, 9, 27.

62. Zhu D, Li G, Xue L and Jiang H, Org. Biomol. Chem, 2013, 11, 4577. [PubMed: 23760313]

63. Davies SS and Guo L, Chem. Phys. Lipids, 2014, 181, 1. [PubMed: 24704586]

64. Li P, Tang B, Xing Y, Li P, Yang G and Zhang L, Analyst, 2008, 133, 1409. [PubMed: 18810289]

65. Wang B, Li P, Yu F, Chen J, Qu Z and Han K, Chem. Commun, 2013, 49, 5790.

66. Tian J, Chen H, Zhuo L, Xie Y, Li N and Tang B, Chem. Eur. J, 2011, 17, 6626. [PubMed: 21590826]

67. Farina M, Rocha JBT and Aschner M, Life Sci, 2011, 89, 555. [PubMed: 21683713]

68. Guo Z, Zhu WH, Zhu MM, Wu XM and Tian H, Chem. Eur. J, 2010, 16, 14424. [PubMed: 21038328]

69. Kim HN, Ren WX, Kim JS and Yoon J, Chem. Soc. Rev, 2012, 41, 3210. [PubMed: 22184584]

70. Han JY and Burgess K, Chem. Rev, 2010, 110, 2709. [PubMed: 19831417]

71. Tang B, Liu X, Xu K, Huang H, Yang G and An L, Chem. Commun, 2007, 3726.

72. Myochin T, Kiyose K, Hanaoka K, Kojima H, Terai T and Nagano T, J. Am. Chem. Soc, 2011, 133, 3401. [PubMed: 21341656]

73. Lee H, Berezin MY, Tang R, Zhegalova N and Achilefu S, Photochem. Photobiol, 2013, 89, 326. [PubMed: 23094959]

74. Lee H, Akers W, Bhushan K, Bloch S, Sudlow G, Tang R and Achilefu S, Bioconjug. Chem, 2011, 22, 777. [PubMed: 21388195]

75. Hilderbrand SA, Kelly KA, Niedre M and Weissleder R, Bioconjug Chem, 2008, 19, 1635. [PubMed: 18666791]

76. Reddie KG and Carroll KS, Curr. Opin. Chem. Biol, 2008, 12, 746. [PubMed: 18804173]

77. Guo Z, Nam S, Park S and Yoon J, Chem. Sci, 2012, 3, 2760.

78. Lee YJ, Chen JC, Amoscato AA, Bennouna J, Spitz DR, Suntharalingam M and Rhee JG, J. Cell. Sci, 2001, 114, 677. [PubMed: 11171373]

79. Wang X, Sun J, Zhang W, Ma X, Lv J, and Tang B, Chem. Sci, 2013, 4, 2551.

80. Strekowski L, Mason JC, Lee H, Say M and Patonay G, J. Heterocyclic Chem, 2004, 41, 227.

81. Kim YM, Choi YD, Weissleder R and Tung CH, Bioorg. Med. Chem. Lett, 2007, 17, 5054. [PubMed: 17664067]

82. Hu C, Sun W, Cao JF, Gao P, Wang JY, Fan JL, Song FL, Sun SG and Peng XJ, Org. Lett, 2013, 15, 4022. [PubMed: 23875747]

83. Bak DW and Weerapana E, Mol. Biosyst, 2015, 11, 678. [PubMed: 25519845]

84. Montserrat M, Morales A, Colell A, Garcia-Ruiz C, Kaplowitz N and Fernandez-Checa JC, Biochim. Biophys. Acta, 2013, 1830, 3317. [PubMed: 23123815]

85. Lim SY, Hong KH, Kim DI, Kwon H and Kim HJ, J. Am. Chem. Soc, 2014, 136, 7018. [PubMed: 24754635]

86. Nani RR, Shaum JB, Gorka AP and Schnermann MJ, Org. Lett, 2015, 17, 302–305. [PubMed: 25562683]

87. Wu X, Shi J, Yang L, Han J and Han S, Bioorg. Med. Chem. Lett, 2014, 24, 314. [PubMed: 24295788]

88. Yang Z, Lee JH, Jeon HM, Han JH, Park N, He Y, Lee H, Hong KS, Kang C and Kim JS, J. Am. Chem. Soc, 2013, 135, 11657. [PubMed: 23865715]

89. Moysan E, Bastiat G and Benoit J-P, Mol. Pharm, 2013, 10, 430. [PubMed: 22978251]

90. Chen Y, Zhu C, Yang Z, Chen J, He Y, Jiao Y, He W, Qiu L, Cen J and Guo Z, Angew. Chem. Int. Ed, 2013, 52, 1688.

91. Yang Z, Liu Z, Chen Y, Wang X, He W and Lu Y, Org. Biomol. Chem, 2012, 10, 5073. [PubMed: 22627395]

92. Shiraishi Y, Nakamura M, Yamamoto K and Hirai T, Chem. Commun, 2014, 50, 11583.

93. Jing CR and Cornish VW, Acc. Chem. Res, 2011, 44, 784. [PubMed: 21879706]

94. Crivat G and Taraska JW, Trends Biotechnol, 2012, 30, 8. [PubMed: 21924508]

95. Yapici I, Lee KS, Berbasova T, Nosrati M, Jia X, Vasileiou C, Wang W, Santos EM, Geiger JH and Borhan B, J. Am. Chem. Soc, 2015, 137, 1073. [PubMed: 25534273]

96. Wang W, Nossoni Z, Berbasova T, Watson CT, Yapici I, Lee KS, Vasileiou C, Geiger JH and Borhan B, Science, 2012, 338, 1340. [PubMed: 23224553]

97. Berbasova T, Nosrati M, Vasileiou C, Wang W, Lee KS, Yapici I, Geiger JH and Borhan B, J. Am. Chem. Soc, 2013, 135, 16111. [PubMed: 24059243]

98. Huang B, Bates M and Zhuang XW, Annu. Rev. Biochem, 2009, 78, 993. [PubMed: 19489737]

99. Schermelleh L, Heintzmann R and Leonhardt H, J. Cell Biol, 2010, 190, 165. [PubMed: 20643879]

100. Sengupta P, Van Engelenburg S and Lippincott-Schwartz J, Dev. Cell, 2012, 23, 1092. [PubMed: 23237943]

101. Sengupta P, van Engelenburg SB and Lippincott-Schwartz J, Chem. Rev, 2014, 114, 3189. [PubMed: 24417572]

102. Chozinski TJ, Gagnon LA and Vaughan JC, FEBS Lett, 2014, 588, 3603. [PubMed: 25010263]

103. van de Linde S and Sauer M, Chem. Soc. Rev, 2014, 43, 1076. [PubMed: 23942584]

104. Heilemann M, Margeat E, Kasper R, Sauer M and Tinnefeld P, J. Am. Chem. Soc, 2005, 127, 3801. [PubMed: 15771514]

105. Bates M, Blosser TR and Zhuang XW, Phys. Rev. Lett, 2005, 94, 108101. [PubMed: 15783528]

106. Rust MJ, Bates M and Zhuang XW, Nat. Methods, 2006, 3, 793. [PubMed: 16896339]

107. Bates M, Huang B, Dempsey GT and Zhuang XW, Science, 2007, 317, 1749. [PubMed: 17702910]

108. Dempsey GT, Bates M, Kowtoniuk WE, Liu DR, Tsien RY and Zhuang XW, J. Am. Chem. Soc, 2009, 131, 18192. [PubMed: 19961226]

109. Shim SH, Xia CL, Zhong GS, Babcock HP, Vaughan JC, Huang B, Wang X, Xu C, Bi GQ and Zhuang XW, Proc. Natl. Acad. Sci. U S A, 2012, 109, 13978. [PubMed: 22891300]

110. Dempsey GT, Vaughan JC, Chen KH, Bates M and Zhuang X, Nat. Methods, 2011, 8, 1027. [PubMed: 22056676]

111. Vaughan JC, Dempsey GT, Sun E and Zhuang XW, J. Am. Chem. Soc, 2013, 135, 1197. [PubMed: 23311875]

112. Vaughan JC, Jia S and Zhuang XW, Nat. Methods, 2012, 9, 1181. [PubMed: 23103881]

113. Deniz E, Tomasulo M, Cusido J, Yildiz I, Petriella M, Bossi ML, Sortino S and Raymo FM, J. Phys. Chem. C, 2012, 116, 6058.

114. Uno S, Kamiya M, Yoshihara T, Sugawara K, Okabe K, Tarhan MC, Fujita H, Funatsu T, Okada Y, Tobita S and Urano Y, Nat. Chem, 2014, 6, 681. [PubMed: 25054937]

115. Byers GW, Gross S and Henrichs PM, Photochem. Photobiol, 1976, 23, 37. [PubMed: 1265127]

116. Samanta A, Vendrell M, Das R and Chang YT, Chem. Commun, 2010, 46, 7406.

117. Lepaja S, Strub H and Lougnot DJ, Z Naturforsch A, 1983, 38, 56.

118. Chen P, Li J, Qian ZG, Zheng DS, Okasaki T and Hayami M, Dyes Pigments, 1998, 37, 213.

119. Kanofsky JR and Sima PD, Photochem. Photobiol, 2000, 71, 361. [PubMed: 10824585]

120. Engel E, Schraml R, Maisch T, Kobuch K, Koenig B, Szeimies RM, Hillenkamp J, Baumler W and Vasold R, Invest. Ophth. Vis. Sci, 2008, 49, 1777.

121. Renikuntla BR, Rose HC, Eldo J, Waggoner AS and Armitage BA, Org. Lett, 2004, 6, 909. [PubMed: 15012062]

122. Toutchkine A, Nguyen DV and Hahn KM, Org. Lett, 2007, 9, 2775. [PubMed: 17583344]

123. Gorka AP, Nani RR, Zhu JJ, Mackem S and Schnermann MJ, J. Am. Chem. Soc, 2014, 136, 14153. [PubMed: 25211609]

124. Toutchkine A, Kraynov V and Hahn KJ, J. Am. Chem. Soc, 2003, 125, 4132. [PubMed: 12670235]

125. Zheng QS, Jockusch S, Zhou Z and Blanchard SC, Photochem Photobiol, 2014, 90, 448. [PubMed: 24188468]

126. Wu X and Zhu W, Chem. Soc. Rev. 2015, DOI 10.1039/C4CS00152D.

127. Widengren J, Chmyrov A, Eggeling C, Lofdahl PA and Seidel CA, J. Phys. Chem. A, 2007, 111, 429. [PubMed: 17228891]

128. Altman RB, Zheng QS, Zhou Z, Terry DS, Warren JD and Blanchard SC, Nat. Methods, 2012, 9, 626.

129. Zheng Q, Juette MF, Jockusch S, Wasserman MR, Zhou Z, Altman RB and Blanchard SC, Chem. Soc. Rev, 2014, 43, 1044. [PubMed: 24177677]

130. van der Velde JHM, Ploetz E, Hiermaier M, Oelerich J, de Vries JW, Roelfes G and Cordes T, Chemphyschem 2013, 14, 4084. [PubMed: 24302532]

131. van der Velde JHM, Oelerich J, Huang JY, Smit JH, Hiermaier M, Ploetz E, Herrmann A, Roelfes G and Cordes T, J. Phys. Chem. Lett, 2014, 5, 3792. [PubMed: 26278749]

132. Warther D, Gug S, Specht A, Bolze F, Nicoud JF, Mourot A and Goeldner M, Bioorg. Med. Chem, 2010, 18, 7753. [PubMed: 20554207]

133. Dore TD and Wilson HC, Chromophores for the Delivery of Bioactive Molecules with Two-Photon Excitation In Photosensitive Molecules for Controlling Biological Function; Chambers JJ, and Kramer RH, R. H., Eds.; Springer Science: New York, 2011; Vol. 55, pp 57–92.

134. Yang YM, Shao Q, Deng RR, Wang C, Teng X, Cheng K, Cheng Z, Huang L, Liu Z, Liu XG and Xing BG, Angew. Chem. Int. Ed, 2012, 51, 3125.

135. Viger ML, Sheng W, Dore K, Alhasan AH, Carling CJ, Lux J, de Gracia Lux C, Grossman M, Malinow R and Almutairi A, ACS Nano, 2014, 8, 4815. [PubMed: 24717072]

136. Brieke C, Rohrbach F, Gottschalk A, Mayer G and Heckel A, Angew. Chem. Int. Ed, 2012, 51, 8446.

137. Ruebner A, Yang ZW, Leung D and Breslow R, Proc. Natl. Acad. Sci. U S A, 1999, 96, 14692. [PubMed: 10611274]

138. Jiang MY and Dolphin D, J. Am. Chem. Soc, 2008, 130, 4236. [PubMed: 18335942]

139. Hossion AML, Bio M, Nkepang G, Awuah SG and You Y, ACS Med. Chem. Lett, 2013, 4, 124. [PubMed: 24900573]

140. Rotaru A and Mokhir A, Angew. Chem. Int. Ed, 2007, 46, 6180.

141. Shell TA, Shell JR, Rodgers ZL and Lawrence DS, Angew. Chem. Int. Ed, 2014, 53, 875.

142. Muzumdar MD, Tasic B, Miyamichi K, Li L and Luo L, Genesis, 2007, 45, 593. [PubMed: 17868096]

143. Nguyen QT and Tsien RY, Nat. Rev. Cancer, 2013, 13, 653. [PubMed: 23924645]
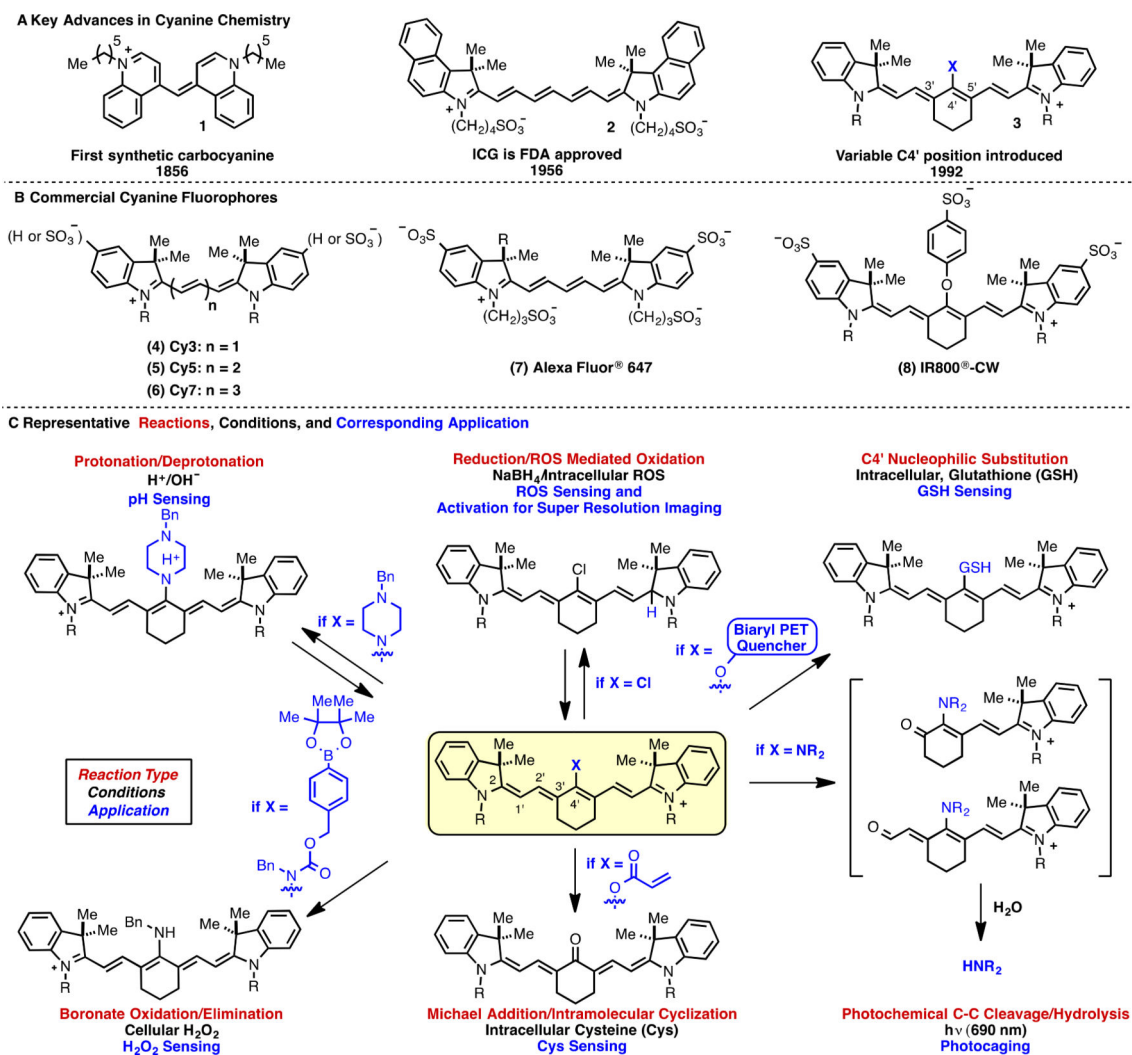
Fig. 1.
(A) Key background, (B) common commercial fluorophores, and (C) overview of cyanine polyene reactivity and applications (Cy3 and Cy5: GE Life Sciences, Alexa 647: Life Technologies, IR800-CW: LI-COR).

Fig. 2.
Cyanine polyene reactivity-based optical sensing approaches.
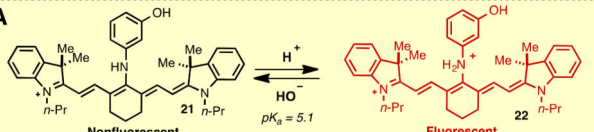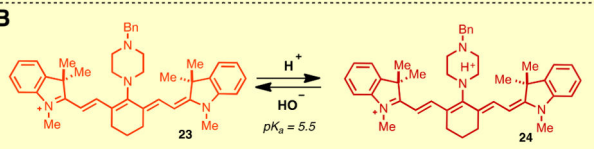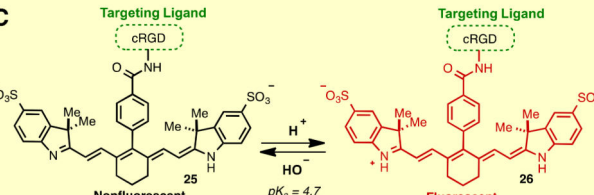
	Reaction	Properties	Application	Lead Reference (Ref. #)
A	Nonfluorescent $\rightleftharpoons$ (H+ / HO−, $pK_a = 5.1$) Fluorescent **21** **22**	**(22)** $\lambda_{abs} = 558$ nm $\lambda_{em} = 615$ nm **10X emission increase from pH 6.5 to 4**	-Intracellular fluoresence microscopy	Tang 2007 (71)
B	Far-red Fluorescence **23** $\rightleftharpoons$ (H+ / HO−, $pK_a = 5.5$) Near-IR Fluorescence **24**	**(23)** $\lambda_{abs} = 686$ nm $\lambda_{em} = 781$ nm **(24)** $\lambda_{abs} = 759$ nm $\lambda_{em} = 789$ nm **~3X change in $\Delta F_{FR}/F_{NIR}$ from pH 9 to 4**	-Intracellular fluoresence microscopy	Myochin 2011 (72)
C	Targeting Ligand cRGD **25** Nonfluorescent $\rightleftharpoons$ (H+ / HO−, $pK_a = 4.7$) Targeting Ligand cRGD **26** Fluorescent	**(26)** $\lambda_{abs} = \sim780$ nm $\lambda_{em} = 795$ nm **>100X emission increase from pH 8 to 4**	-*In vivo* imaging of xenograft and orthotopic tumor models	Lee 2011 (74)

Fig. 3.
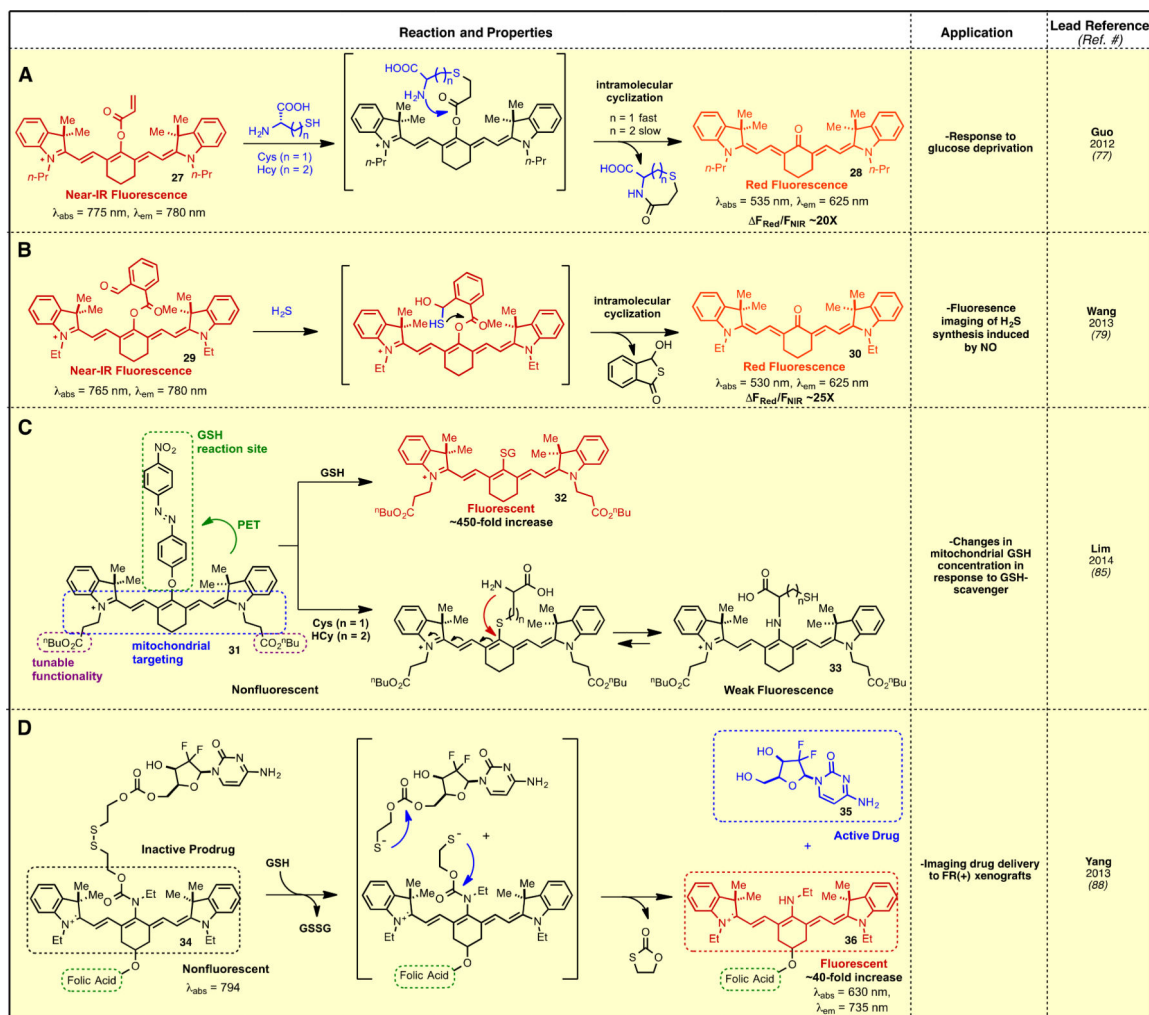pH-Sensing approaches.

Fig. 4.
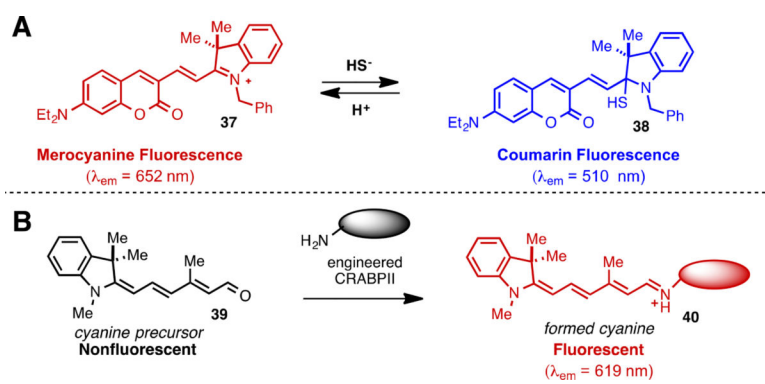Thiol sensing methods.

Fig. 5.
(A) Coumarin/cyanine hybrid for H_2S sensing and (B) *in situ* cyanine formation with engineered CRABPII protein.
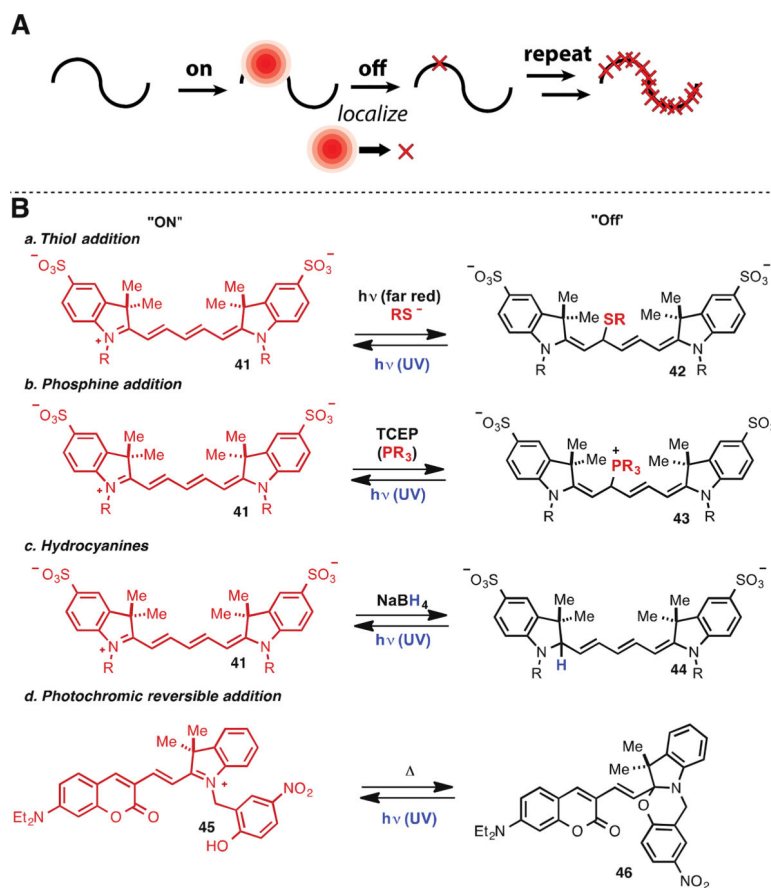
Fig. 6.
(A) General scheme for switching-dependent super resolution microscopy and (B) cyanine switching reactivity.
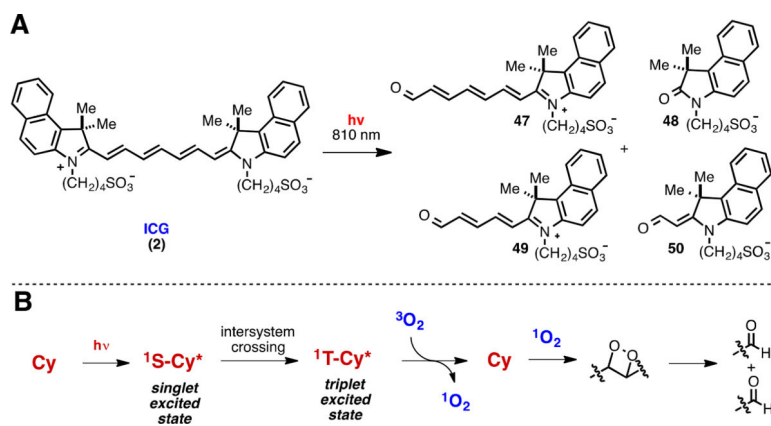
A

B

Fig. 7.
(A) ICG photobleaching products and (B) general singlet-oxygen photooxidation mechanism.

Fig. 8.
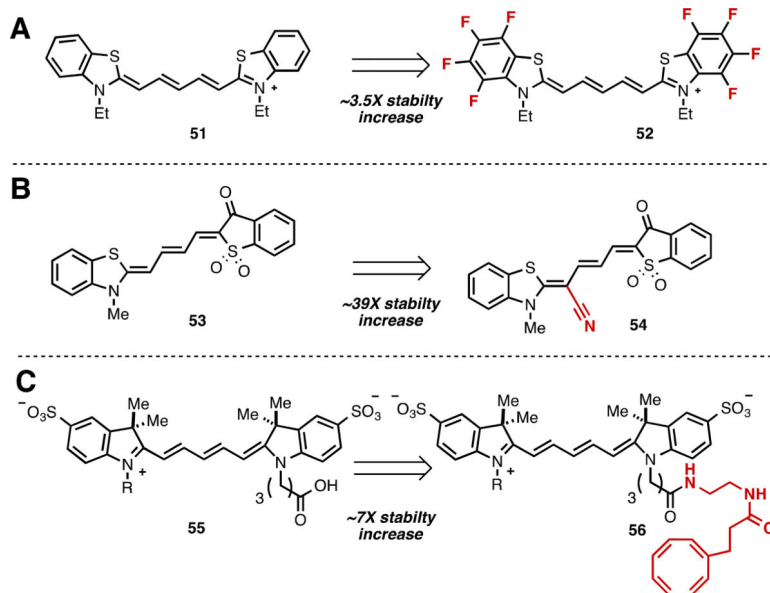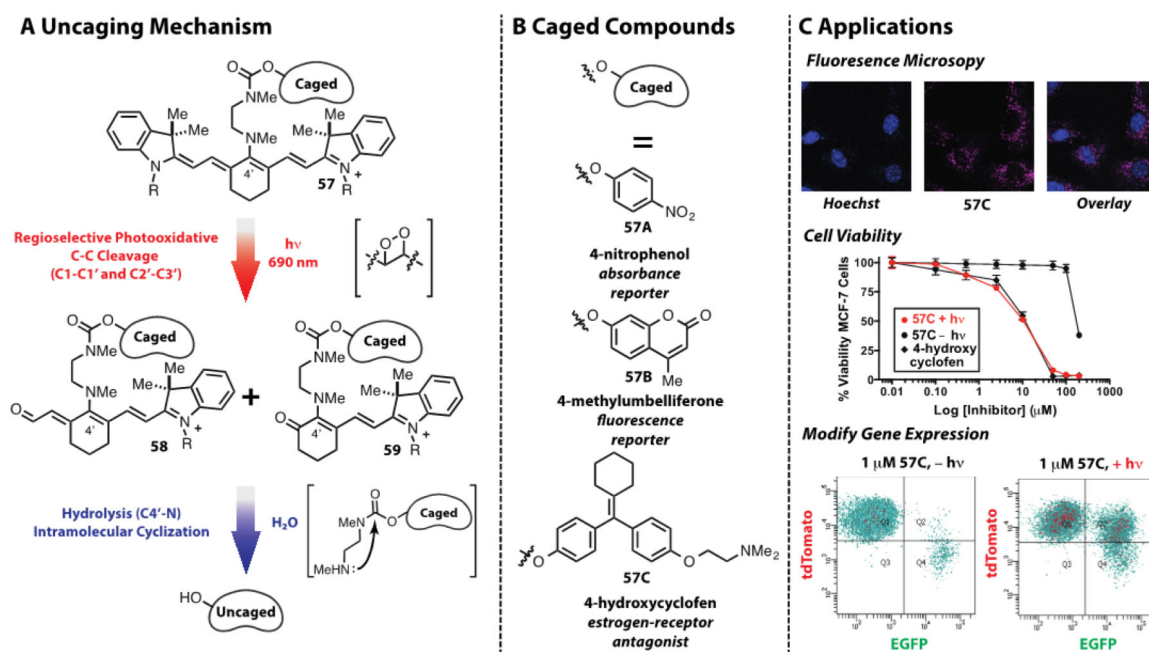Strategies for improving cyanine photostability.

Fig. 9.
(A) Near-IR cyanine uncaging mechanism, (B) caged compounds, and (C) applications.